

PAPER • OPEN ACCESS

Potts Model with Competing Binary-Ternary-Quaternary Interactions on Cayley Tree

To cite this article: N Ganikhodjaev *et al* 2020 *J. Phys.: Conf. Ser.* **1489** 012023

View the [article online](#) for updates and enhancements.



IOP | ebooks™

Bringing together innovative digital publishing with leading authors from the global scientific community.

Start exploring the collection—download the first chapter of every title for free.

Potts Model with Competing Binary-Ternary-Quaternary Interactions on Cayley Tree

N Ganikhodjaev*, M H Mohd Rodzhan and N F I Omar Baki

Department of Computational and Theoretical Sciences, Faculty of Science,
International Islamic University Malaysia. 25200 Kuantan. Pahang, Malaysia.

*E-mail: gnasir@iiium.edu.my

Abstract. We study the phase diagrams for the Potts model with competing binary, ternary and quaternary interactions on Cayley tree of order 2. At vanishing temperature T , the phase diagram is fully determined for all values of competing binary, ternary and quaternary interactions. We extend the results (for the case $J_q = 0$) obtained by Ganikhodjaev et. al. [9]. The results show that the appearance of addition phases: antiferromagnetic and Period 6, in the case of nonzero quaternary interactions for several ranges. Then, we investigate the modulated phase, with the phase being indicated by many different types of commensurate and incommensurate phases by plotting the wavevectors versus temperature. Lastly, the Lyapunov exponent is used to verify the stability of the periods.

1. Introduction

In statistical mechanics, the lattice spin system is well known as the large class of systems, since this system is an idealized version of magnets. The lattice spin system can simply be thought as the angular momentum vector of spinning particle, and so can be represented as an arrow. The structure of the lattice also plays an important role in examinations of spins systems. The reason is many many-body physical systems of interest can effectively be treated as being on lattice, besides it makes the models easier to formulate, since the probabilities and other the physical quantities are defined in terms of sums instead of integrals.

Ising model is one particular mathematical model in statistical mechanics is used to study of two-way translation between the behavior of the individual element (microscopic properties) and the properties of the system as a whole (macroscopic properties). The Potts model, which was introduced by Potts in 1952, was presented as a generalization of the Ising model to more than two components and is the most studied model in recent years because of its wide practical applications and theoretical interest [1]. The idea of Potts model originates from a representation of the Ising model as interacting spins which can be either parallel or anti-parallel [2].

One of the important advantages of considering models on Bethe lattice also known as Cayley Tree, is that no approximations have to be made and the calculations can be carried out with high accuracy. Then, the simplest way of resolving the system problems can come up with the solution. These problems can be solved by using mean-field theory in order to describe phase transition in the phase diagrams and also to study the behavior of large and complex stochastic models by studying a simpler model on lattice. Studies of such model may lead to a discovery of more



realistic systems with similar properties. Potts model as a generalization of the Ising model on Cayley tree with competing interactions, appeared in pioneering work of Vannimenus, has recently been studied extensively by ([1,3,4,7,8,9,10]).

For solving the problem on a tree is much easier to understand mathematically rather than the set of all lattice points and is equivalent to the standard Bethe-Peierls theory [2]. In recent years, many researchers have studied the phase diagrams corresponding to Ising models (see [5,6,11]) and also 3-state lattice model (Potts model) on Cayley tree (see [7,8,9,10]). The approach is used to study the phase diagram of lattice model on Cayley tree is to describe the morphology of the phases, the stability of the phases, the transitions from one phase to another and corresponding transition lines. The producing the phase diagram is followed by studying the behavior of recurrence systems of model.

In this paper, we consider the Potts model with competing interactions up to third nearest-neighbor generations on Cayley tree of order two. We derive the recurrent equations from partition functions that are defined on Cayley tree. Then, we study the behavior of the recurrent equations of system for producing the phase diagrams. Lastly, we investigate in detail the modulated phases by plotting the graph of wavevectors versus temperature and verify the stability of the periods by studying the Lyapunov exponent. This research is an extension work that considered in [9].

2. The Model Hamiltonian

In this section, we are considering the Potts model with three competing interactions on semi-infinite Cayley tree Γ_+^k of k -th order. Now, let us give some definitions to construct the model.

A Cayley tree Γ^k of order $k \geq 1$ is an infinite tree, i.e., a graph without cycles with exactly $k + 1$ edges issuing from each vertex. Let denote the Cayley tree as $\Gamma^k = (V, \Lambda)$, where V is the set of vertices of Γ^k , Λ is the set of edges of Γ^k . Two vertices x and y , where $x, y \in V$ are called *nearest-neighbor* if there exists an edge $l \in \Lambda$ connecting them, which is denoted by $l = \langle x, y \rangle$. The distance $d(x, y)$, $x, y \in V$, on the Cayley tree Γ^k , is the number of edges in the shortest path from x to y . For a fixed $x^0 \in V$ we set $W_n = \{x \in V | d(x, x^0) = n\}$, $V_n = \{x \in V | d(x, x^0) \leq n\}$, and L_n denotes the set of edges in V_n . The fixed vertex x^0 is called the 0 -th level and the vertices in W_n are called the n -th level. For the sake of simplicity we put $|x| = d(x, x^0)$, $x \in V$. Two vertices $x, y \in V$ are called *second nearest-neighbor* if $d(x, y) = 2$. The second nearest-neighbor vertices x and y are called *prolonged second nearest-neighbor* if $|x| \neq |y|$ and is denoted by $> \tilde{x}, \tilde{y} <$. The second nearest-neighbor vertices $x, y \in V$ that are not prolonged are called *one-level second nearest-neighbor* since $|x| = |y|$ and are denoted by $> \bar{x}, \bar{y} <$. Two vertices $x, y \in V$ are called *third nearest-neighbor* if $d(x, y) = 3$. The third nearest-neighbor vertices x and y are called *prolonged third nearest-neighbor* and is denoted by $< \tilde{x}, \tilde{y} >$ if $x \in W_n$ and $y \in W_{n+3}$. The third nearest-neighbor vertices $x, y \in V$ that are not prolonged are called *two-level third nearest-neighbor* is denoted by $< \tilde{x}, \tilde{y} >_3$, respectively $x \in W_{n+1}$ and $y \in W_n$; i.e. they belong to the different branches of Cayley tree.

We write $x < y$ if the path from x^0 to y goes through x . We call the vertex y a direct successor of x , if $y > x$ and x, y are nearest neighbors. The set of the direct successors of x is denoted by $S(x)$, i.e., if $x \in W_n$, then $S(x) = \{y_i \in W_{n+1} | d(x, y_i) = 1, i = 1, \dots, k\}$. We observe that for any vertex $x \neq x^0$, x has k direct successors and x^0 has $k+1$. In this case, we will consider a semi-infinite Cayley tree Γ_+^k of k -th order, i.e., an infinite graph without cycles with $k+1$ edges issuing from each vertex except for x^0 which has only k edges, that is $|S(x)| = 2$ (Cayley tree of order 2) for any $x \in V$.

In the case of Potts Model with spin values in $\phi = \{1, 2, 3\}$, the relevant Hamiltonian with competing binary, ternary and quaternary interactions have the forms

$$H(\sigma) = -J_1 \sum_{\langle x,y \rangle} \delta_{\sigma(x)\sigma(y)} - J_t \sum_{\langle x,y,z \rangle} \delta_{\sigma(x)\sigma(y)\sigma(z)} - J_q \sum_{\langle x,y,z,w \rangle} \delta_{\sigma(x)\sigma(y)\sigma(z)\sigma(w)} \quad (1)$$

where the first summation is over all first nearest-neighbor binary interactions, the second summation is over all second nearest-neighbor ternary interactions and the third summation is over all third nearest-neighbor quaternary interactions. Here, $J_1, J_t, J_q \in \mathbb{R}$ are coupling constants, the symbol δ in first, second and third sum is the usual Kronecker symbol that is defined as:-

$$\begin{aligned} \delta_{\sigma(x)\sigma(y)} &= \begin{cases} 1, & \text{if } \sigma(x) = \sigma(y), \\ 0, & \text{if otherwise,} \end{cases} \\ \delta_{\sigma(x)\sigma(y)\sigma(z)} &= \begin{cases} 1, & \text{if } \sigma(x) = \sigma(y) = \sigma(z), \\ 0, & \text{if otherwise,} \end{cases} \\ \delta_{\sigma(x)\sigma(y)\sigma(z)\sigma(w)} &= \begin{cases} 1, & \text{if } \sigma(x) = \sigma(y) = \sigma(z) = \sigma(w), \\ 0, & \text{if otherwise.} \end{cases} \end{aligned} \quad (2)$$

The spin variables $\sigma(x)$ assume the values 1, 2 and 3. Noting that, if $J_q = 0$ then the Hamiltonian (1) is reduced to Hamiltonian in [9]. The phase diagram for $J_q = 0$ has a very simple structure that consists of four phases: paramagnetic, ferromagnetic, antiphase and modulated phases.

3. Basic Equations

Next, we want to study the phase diagrams of Potts Model with competing binary-ternary-quaternary interaction on the same branch of second order of Cayley Tree. In order of that, we are going to derive the recurrence equations from the partition functions that are defined on second order of Cayley Tree.

By following the ideas of producing the recurrent equations in [11], we consider the relation of the partition function on V_{n+1} to the partition function on its subsets V_n . Then, the recurrent equations indicate how their influence propagates down the tree by giving the initial conditions on V_2 . We extend one level up of successive generations from the previous case done in [9] by taking into account the partial partition functions for all possible configurations of the spins in three successive generations.



Figure 1. (a) A double-trunk Cayley tree $\Gamma_{(x^0,y,z)}^2$, which from x^0 emanates single edge $\langle x^0, y \rangle$ and from vertex y emanates two edges $\langle x^0, y \rangle \langle y, z \rangle$; (b) A configuration on $V_3^{(x^0,y,z)}$ with fixed boundary conditions $\bar{\sigma}^2 \equiv 1$.

Now, we will consider the partition functions $Z^{(n)}(\sigma(x^0), \sigma(y), \sigma(z); \bar{\sigma}^n)$ on $V_n^{(x^0,y,z)}$ with the configuration on double-trunk Cayley tree (x^0, y, z) is shown in the Figure 1(a), and given the boundary condition $\bar{\sigma}^n$. By considering all partition functions on $V_n^{(x^0,y,z)}$ with fixed V_2 , under the boundary conditions $\bar{\sigma}^n \equiv 1$, then we can show that there are 27 partition functions defined on a double-trunk Cayley tree. We assume that $J_t \neq 0$ and $J_q \neq 0$, and we choose the boundary condition $\bar{\sigma}^n \equiv 1$. If we consider all partition functions in volume $V_{n+1}^{(x^0,y,z)}$ is shown in Figure 1(b), under the boundary condition $\bar{\sigma}^n \equiv 1$, then we have

$$\begin{aligned} Z^{(n)}(2,1,2) &= Z^{(n)}(1,3,2) = Z^{(n)}(1,2,3) = Z^{(n)}(2,1,3) \\ &= Z^{(n)}(2,3,2) = Z^{(n)}(3,1,2) = Z^{(n)}(3,1,3) = Z^{(n)}(3,2,3); \\ Z^{(n)}(1,1,2) &= Z^{(n)}(1,1,3) = Z^{(n)}(2,2,3) = Z^{(n)}(3,3,2); \\ Z^{(n)}(1,2,1) &= Z^{(n)}(1,3,1) = Z^{(n)}(2,3,1) = Z^{(n)}(3,2,1); \\ Z^{(n)}(3,2,2) &= Z^{(n)}(1,3,3) = Z^{(n)}(2,3,3) = Z^{(n)}(1,2,2); \\ Z^{(n)}(2,1,1) &= Z^{(n)}(3,1,1); \quad Z^{(n)}(2,2,1) = Z^{(n)}(3,3,1); \\ &\text{and} \\ Z^{(n)}(3,3,3) &= Z^{(n)}(2,2,2). \end{aligned}$$

Then, 27 partition functions can be reduced to 8 variables $Z^{(n)}(1,1,1)$, $Z^{(n)}(1,1,2)$, $Z^{(n)}(1,2,1)$, $Z^{(n)}(2,1,1)$, $Z^{(n)}(2,1,2)$, $Z^{(n)}(2,2,1)$, $Z^{(n)}(3,2,2)$, $Z^{(n)}(3,3,3)$. We define for convenience the following variables:

$$\begin{aligned} u_1^{(n)} &= \sqrt[4]{Z^{(n)}\left(\sigma_n \begin{pmatrix} 1 & 1 & 1 & 1 \\ & 1 & 1 & \\ & & 1 & \\ & & & 1 \end{pmatrix}\right)}, & u_2^{(n)} &= \sqrt[4]{Z^{(n)}\left(\sigma_n \begin{pmatrix} 2 & 2 & 2 & 2 \\ & 1 & 1 & \\ & & 1 & \\ & & & 1 \end{pmatrix}\right)}, \\ u_3^{(n)} &= \sqrt[4]{Z^{(n)}\left(\sigma_n \begin{pmatrix} 1 & 1 & 1 & 1 \\ & 2 & 2 & \\ & & 1 & \\ & & & 1 \end{pmatrix}\right)}, & u_4^{(n)} &= \sqrt[4]{Z^{(n)}\left(\sigma_n \begin{pmatrix} 1 & 1 & 1 & 1 \\ & 1 & 1 & \\ & & 2 & \\ & & & 1 \end{pmatrix}\right)}, \\ u_5^{(n)} &= \sqrt[4]{Z^{(n)}\left(\sigma_n \begin{pmatrix} 2 & 2 & 2 & 2 \\ & 1 & 1 & \\ & & 2 & \\ & & & 1 \end{pmatrix}\right)}, & u_6^{(n)} &= \sqrt[4]{Z^{(n)}\left(\sigma_n \begin{pmatrix} 1 & 1 & 1 & 1 \\ & 2 & 2 & \\ & & 2 & \\ & & & 1 \end{pmatrix}\right)}, \\ u_7^{(n)} &= \sqrt[4]{Z^{(n)}\left(\sigma_n \begin{pmatrix} 2 & 2 & 2 & 2 \\ & 2 & 2 & \\ & & 3 & \\ & & & 1 \end{pmatrix}\right)}, & \text{and } u_8^{(n)} &= \sqrt[4]{Z^{(n)}\left(\sigma_n \begin{pmatrix} 3 & 3 & 3 & 3 \\ & 3 & 3 & \\ & & 3 & \\ & & & 1 \end{pmatrix}\right)}. \end{aligned} \tag{3}$$

Establishing the following recursive relations is straightforward. The primed variables (u'_1, \dots, u'_8) correspond to $(u_1^{(n+1)}, \dots, u_8^{(n+1)})$, with $a = \exp\left(\frac{J_1}{k_B T}\right)$, $b = \exp\left(\frac{J_t}{k_B T}\right)$ and $c = \exp\left(\frac{J_q}{k_B T}\right)$ can be obtained as follows:-

$$\begin{aligned} u'_1 &= \sqrt{a} b \left(c u_1^{(n)} + 2 u_2^{(n)} \right)^2, & u'_2 &= \sqrt{a} \left(u_3^{(n)} + u_5^{(n)} + u_7^{(n)} \right)^2, & u'_3 &= \left(u_4^{(n)} + 2 u_5^{(n)} \right)^2, \\ u'_4 &= \left(u_1^{(n)} + 2 u_2^{(n)} \right)^2, & u'_5 &= \left(u_3^{(n)} + u_5^{(n)} + u_7^{(n)} \right)^2, & u'_6 &= \sqrt{a} \left(u_4^{(n)} + 2 u_5^{(n)} \right)^2, \\ u'_7 &= \left(u_2^{(n)} + u_6^{(n)} + u_8^{(n)} \right)^2 & \text{and} & & u'_8 &= \sqrt{a} b \left(u_2^{(n)} + u_6^{(n)} + c u_8^{(n)} \right)^2. \end{aligned}$$

Noting that $u'_2 = \sqrt{a} u'_5$ and $u'_6 = \sqrt{a} u'_3$, then, only six independent variables remain, and the recurrence system takes the simpler form:

$$\begin{aligned} u'_1 &= \sqrt{a} b \left(c u_1^{(n)} + 2 \sqrt{a} u_5^{(n)} \right)^2, & u'_3 &= \left(u_4^{(n)} + 2 u_5^{(n)} \right)^2, \\ u'_4 &= \left(u_1^{(n)} + 2 \sqrt{a} u_5^{(n)} \right)^2, & u'_5 &= \left(u_3^{(n)} + u_5^{(n)} + u_7^{(n)} \right)^2, \\ u'_7 &= \left(\sqrt{a} u_5^{(n)} + \sqrt{a} u_3^{(n)} + u_8^{(n)} \right)^2 & \text{and} & & u'_8 &= \sqrt{a} b \left(\sqrt{a} u_5^{(n)} + \sqrt{a} u_3^{(n)} + c u_8^{(n)} \right)^2. \end{aligned}$$

Then, the total partition function is given in terms of $(u_i^{(n)})$ by:

$$\begin{aligned} Z^{(n)} &= \left[\left(u_1^{(n)} + 2 \sqrt{a} u_5^{(n)} \right)^2 + 2 \left(u_3^{(n)} + u_5^{(n)} + u_7^{(n)} \right)^2 \right]^2 \\ &+ 2 \left[\left(u_8^{(n)} + \sqrt{a} \left(u_3^{(n)} + u_5^{(n)} \right) \right)^2 + \left(u_3^{(n)} + u_5^{(n)} + u_7^{(n)} \right)^2 + \left(u_4^{(n)} + 2 u_5^{(n)} \right)^2 \right]^2. \end{aligned}$$

Note that in the paramagnetic phase (high symmetry phase), we have $u_1 = u_8$, $u_4 = u_7$ and $u_3 = u_5$ [11]. Thus, for presenting the phase diagram, the possible choice of reduced variables is:-

$$x_1 = \frac{u_3 + u_5}{u_1 + u_8}; \quad x_2 = \frac{u_4 + u_7}{u_1 + u_8}; \quad y_1 = \frac{u_1 - u_8}{u_1 + u_8}; \quad y_2 = \frac{u_3 - u_5}{u_1 + u_8}; \quad y_3 = \frac{u_4 - u_7}{u_1 + u_8}. \quad (4)$$

Lastly, for general system of recurrent equations for the Potts model, equation (1), on a Cayley tree of order 2 can be produced as the following:

$$\begin{aligned} x'_1 &= \frac{1}{b \cdot A} [x_2^2 + 4x_2x_1 - 2x_2y_2 + y_3^2 - 2y_3y_2 + 4x_1^2 - 4x_1y_2 + 2y_2^2], \\ x'_2 &= \frac{1}{b \cdot A} [1 + 4\sqrt{a} x_1 - 2\sqrt{a} y_2 + y_1^2 - 2\sqrt{a} y_2y_1 + 4ax_1^2 - 4ax_1y_2 + 2ay_2^2], \\ y'_1 &= \frac{-2}{A} [-\sqrt{a} c^2 y_1 + acy_2 - 2acy_1x_1 + acy_1y_2 + 2a^{3/2}x_1y_2 - a^{3/2}y_2^2], \\ y'_2 &= \frac{-2}{b \cdot A} [-x_2y_3 + x_2y_2 - 2y_3x_1 + y_3y_2 + 2x_1y_2 - y_2^2], \\ y'_3 &= \frac{2}{b \cdot A} [y_1 - \sqrt{a} y_2 + 2\sqrt{a} y_1x_1 - \sqrt{a} y_1y_2 - 2ax_1y_2 + ay_2^2] \end{aligned} \quad (5)$$

where,

$$A = \left(\sqrt{a} c^2 + 4acx_1 - 2acy_2 + \sqrt{a} c^2 y_1^2 - 2acy_1y_2 + 4a^{3/2}x_1^2 - 4a^{3/2}x_1y_2 + 2a^{3/2}y_2^2 \right).$$

The average magnetization m for the N th generation is given by

$$m = \frac{B^2 - C^2}{C^2 + 2B^2} \quad (6)$$

where,

$$B = 1 - 2y_1 + 4\sqrt{a}x_1 + y_1^2 - 4y_1\sqrt{a}x_1 + 4ax_1^2 + 2x_2^2 + 8x_1x_2 + 2y_3^2 + 8x_1^2 - 8x_1y_2 + 4y_2^2 - 4x_2y_2 - 4y_2y_3;$$

$$C = 1 + 2y_1 + 4\sqrt{a}x_1 - 4\sqrt{a}y_2 + y_1^2 + 4y_1\sqrt{a}x_1 - 4y_1\sqrt{a}y_2 + 4ax_1^2 - 8ax_1y_2 + 4ay_2^2 + 2x_2^2 - 4x_2y_3 + 8x_1x_2 + 2y_3^2 - 8x_1y_3 + 8x_1^2.$$

4. Morphology of Phase Diagrams

Now, we are going to produce the phase diagrams by studying the detailed behavior of the recurrence system of equations. This can be achieved numerically in a straightforward fashion. Starting from the initial conditions:-

$$x_1^{(1)} = \frac{a^2 + 1}{a^2b(a^2b^2c^2 + 1)}; \quad x_2^{(1)} = \frac{a^2b^2 + 1}{ab(a^2b^2c^2 + 1)};$$

$$y_1^{(1)} = \frac{a^2b^2c^2 - 1}{(a^2b^2c^2 + 1)}; \quad y_2^{(1)} = \frac{a^2 - 1}{a^2b(a^2b^2c^2 + 1)}; \quad y_3^{(1)} = \frac{a^3b^2 - a}{a^2b(a^2b^2c^2 + 1)}. \quad (7)$$

that corresponds to boundary condition $\bar{\sigma}^n \equiv 1$, one iterates the recurrence relations in equation (5) and observes the behavior after a large number of iterations. If its attractor is a fixed point $(x_1^*, x_2^*, y_1^*, y_2^*, y_3^*)$, then it corresponds to a paramagnetic phase when $y_1^* = y_2^* = y_3^* = 0$, or corresponds to a ferromagnetic phase when $y_1^*, y_2^*, y_3^* \neq 0$. The finite attractor corresponds to periodic (commensurate) phase and infinite attractor corresponds to aperiodic (incommensurate) phase.

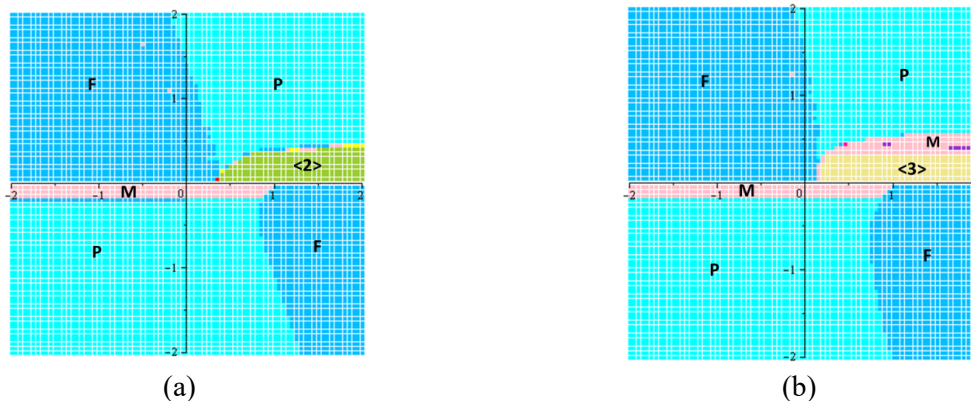


Figure 2. (a) Phase diagrams of α vs β for the model with $J_q = 0$; (b) Phase diagrams of α vs $-\delta$ for the model with $J_t = 0$

Let $\alpha = k_B T/J_1$, $\beta = -J_t/J_1$ and $\delta = J_q/J_1$. The phase diagram in the Figure 2(a) showed the result that was done by [9] for the case $J_q = 0$ in equation (1). Then, the extension results from the previous case, the phase diagrams are shown in Figure 2(b) and Figure 3 if we considered for nonzero J_q case. (Note that P - paramagnetic, F - ferromagnetic, AF - antiferromagnetic, <3> - antiphase with period 3, <2> - antiphase with period 2 and M - modulated phase).

The phase diagram for the case $J_q = 0$, consists of ferromagnetic, paramagnetic, a periodic $(- - ++)$ antiphase $\langle 2 \rangle$ and modulated phase with $p > 12$, where these phases meet at a nonzero temperature multicritical point [9]. For extension case ($J_q \neq 0$), the resultant phase diagrams in the Figure 3 show the appearance of a periodic $(+ - + - + -)$ antiphase $\langle 3 \rangle$ in addition to the previous one and also phase of antiferromagnetic for $\delta = -2$ and $\delta = 1$.

However, by considering the case for nonzero J_q and fixed the parameter $J_t = 0$ for this model, then the resultant phase diagram as shown in the Figure 2(b) shows that the replacement phase of antiphase $\langle 3 \rangle$ with period 6 to the antiphase $\langle 2 \rangle$ with period 4 as shown in the Figure 2(a) (for the case nonzero J_t and fixed the parameter $J_q = 0$).

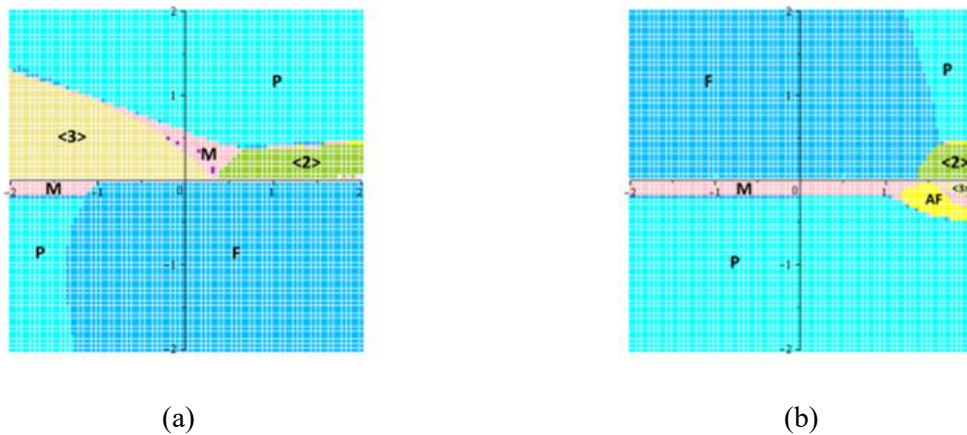


Figure 3. (a) Phase diagrams of α vs β for the model with $\delta = -2$; (b) Phase diagrams of α vs β for the model with $\delta = 1$.

5. Variation of Wavevector with Temperature and The Lyapunov Exponent

In this section, we are going to study the set modulated phase in detail by conducting an investigation on the wavevector by varying the temperature and the Lyapunov exponent.

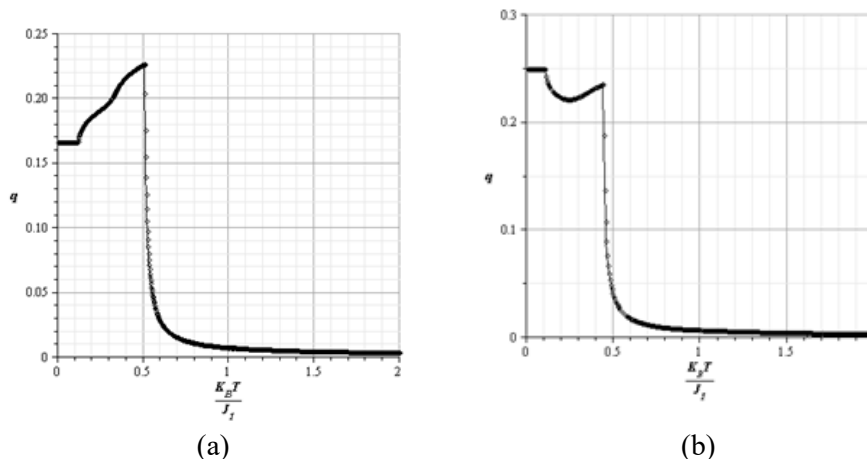


Figure 4. Variation of the wavevector q versus temperature: (a) $\beta = 0.2$; (b) $\beta = 0.4$ with $\delta = -2$.

The definition of the wavevector that is convenient for numerical purpose is

$$q = \lim_{N \rightarrow \infty} \frac{n(N)}{2N},$$

where $n(N)$ is the number of times the magnetization in equation (6) changes sign during N successive iterations [11]. A graph of q versus α is drawn in the Figure 4 for (a) $\beta = 0.2$ and (b) $\beta = 0.4$ at the fixed value of $\delta = -2$. By referring to the phase diagram in the Figure 3(a), one can see that the value of q starts with $q \approx 0.1667$ in the Figure 4(a), is indicating to the phase of antiphase $\langle 3 \rangle$, while in the Figure 4(b) the value of q starts with $q = 0.25$ is indicating to phase of antiphase $\langle 2 \rangle$. These phases are stable and it can be proved by computing the Lyapunov exponent, which is negative value. We investigate the modulated phase, with the phase being indicated by many different values of q . According to the general theory, the present of main locking steps can be located by investigating a function of $q(T)$ in detail. This interval can be very narrow; moreover, the distinction between long-periodic cycles and truly aperiodic solutions is difficult to achieve numerically. The answer to this problem consists in computing the Lyapunov exponent associated with the trajectory of the system, as discussed and presented in Reference 11.

The Lyapunov exponent is needed to show a behavior which is the logarithm of the largest eigenvalue has a simple fixed point (attractor). The Lyapunov exponent also tells us whether an infinitesimal perturbation of the initial conditions will have an infinitesimal effect (negative exponent) or will lead to a totally different trajectory (positive exponent). The calculation of the Lyapunov exponent for Potts model can be summarized as follows: the recurrent equations in equation (5) are linearized around the successive points of the trajectory, yielding linear recurrent equations for the perturbations $(\delta x_1, \delta x_2, \delta y_1, \delta y_2, \delta y_3)$ (see the discussion detailed in Reference 11). In matrix form, one has

$$V_{k+1} = \begin{pmatrix} \delta x_1' \\ \delta x_2' \\ \delta y_1' \\ \delta y_2' \\ \delta y_3' \end{pmatrix} = L_k \begin{pmatrix} \delta x_1 \\ \delta x_2 \\ \delta y_1 \\ \delta y_2 \\ \delta y_3 \end{pmatrix},$$

where the matrix L_k depends on the iteration step. The Lyapunov exponent λ is obtained as

$$\lambda = \lim_{N \rightarrow \infty} \frac{1}{N} \log(\|V_N\|),$$

where $\|V_N\|$ denotes the norm of the vector V . Stable limit cycles may exist only for negative exponents.

In the Figure 5, at fixed value of $\delta = -2$, the value of $\beta = 0.2$ was chosen because q is close to $2/11$ and $5/29$. The stability intervals for these values of q are rather narrow: from $\alpha \in (0.1620, 0.1657)$ (see the Figure 5(c)), and $\alpha \in (0.1250, 0.1253)$ (see the Figure 5(d)) respectively. Next, we calculate the Lyapunov exponent for verifying the stability of the phases in the set of modulated phases. Then, every region of negative λ is numerically found to coincide with the stability domain of a given cycle. So, for this case, the results are obtained for a cycle of period with $N = 10000$ iteration steps (the initial 1000 steps are discarded for each value of T , as discussed in Reference 11).

As the result in the Figure 5(a) shows that the present of the variation of Lyapunov exponent for a stability cycle of period 11 for $\beta = 0.2$ with the fixed value of $\delta = -2$. Moreover, we show a stability cycle of period 29 in the Figure 5(b) for the same case but the different regions of α .

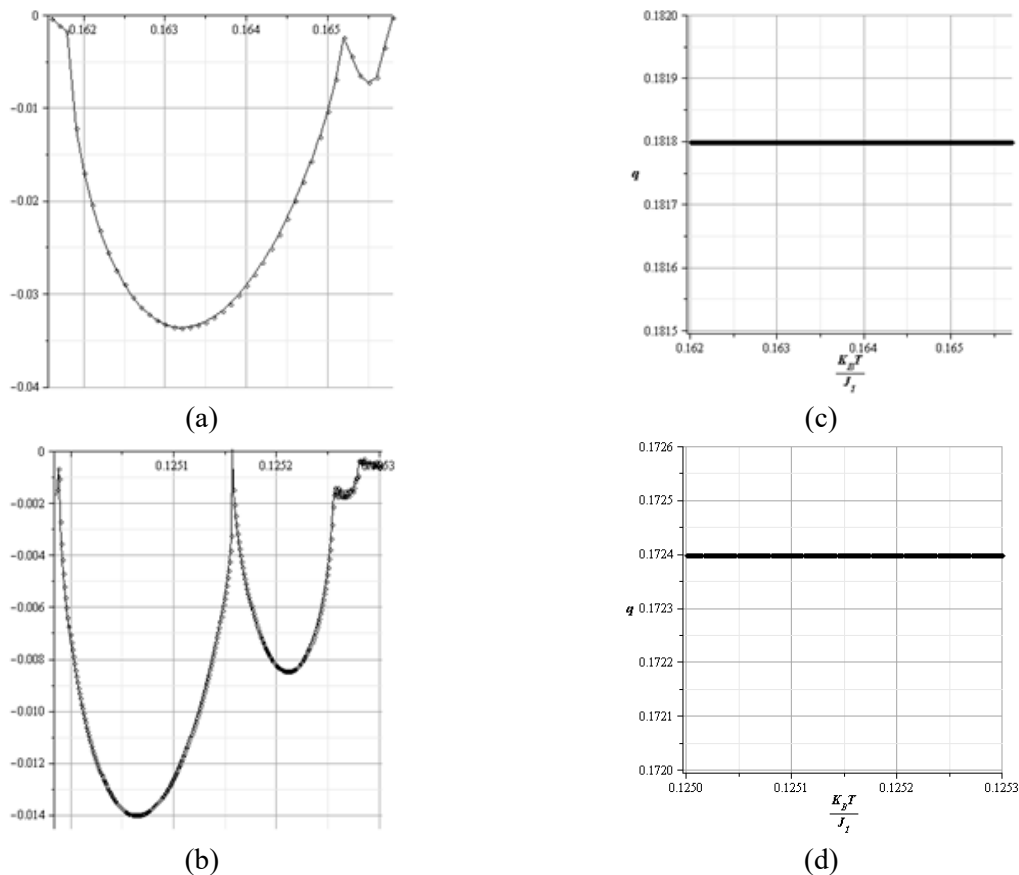
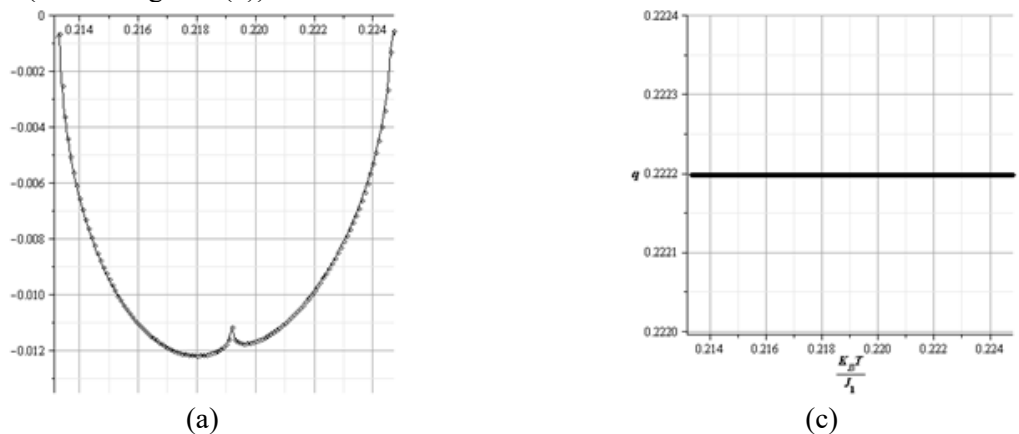


Figure 5. (a) and (b) Variation of the Lyapunov exponent λ versus temperature for $\beta = 0.2$ with fixed value of $\delta = -2$ in the regions of commensurate steps (c) $q \approx 2/11$ and (d) $q \approx 5/29$ enlarged from Fig. 4(a), corresponding to Fig. 3(a).

Then, for the same fixed value of δ as stated previously, the value of $\beta = 0.4$ was selected and the result finds that q is close to $2/9$ and $4/17$ as are shown in the Figure 6. By using the same way, the stability intervals for these values of q are rather narrow: from $\alpha \in (0.2133, 0.2248)$ (see the Figure 6(c)), and $\alpha \in (0.1248, 0.1255)$ (see the Figure 6(d)) respectively. For the verification of the stability of the phases for this case, the results are shown in the Figure 6(a) and Figure 6(b). Then, we found that the stable regions with $q \approx 2/9$ (see the Figure 6(c)), corresponding to a limit of cycle of period 9 (see the Figure 6(a)) and for $q \approx 4/17$ (see the Figure 6(d)), corresponding to a limit cycle of period 17 (see the Figure 6(b)).



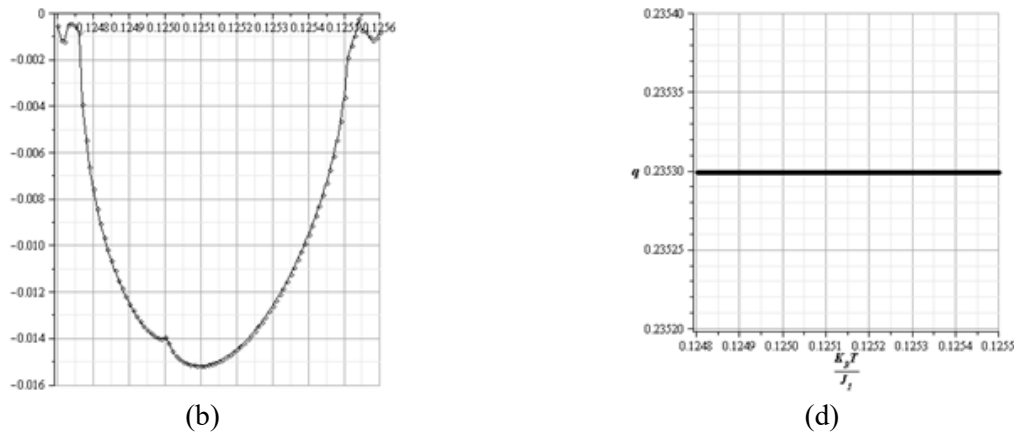


Figure 6. (a) and (b) Variation of the Lyapunov exponent λ versus temperature for $\beta = 0.4$ with fixed value of $\delta = -2$ in the regions of commensurate steps (c) $q \approx 2/9$ and (d) $q \approx 4/17$ enlarged from the Figure 4(b), corresponding to the Figure 3(a).

Numerically, every region of negative λ is found to coincide with the stability domain of a given cycle. Finally, all stable limit cycles can be confirmed by checking the trajectory of the system in equation (5) corresponding to the given interval of α , as presented in the Figure 5 and the Figure 6.

6. Conclusion

In this research, we have considered Potts Model with competing binary-ternary-quaternary interaction on Cayley tree of second order. We produced the general recurrence system of equations, and study its behavior for producing the phase diagrams for extension result obtained by [9]. In resultant phase diagrams, we found a new antiphase $\langle 3 \rangle$ with period 6 and antiferromagnetic phase in addition to the expected paramagnetic, ferromagnetic, antiphase $\langle 2 \rangle$ with period 4 and modulated phases. Then, if we considered the case of nonzero J_q and fixed the parameter $J_t = 0$, the phase diagram shows that the replacement phase of antiphase $\langle 3 \rangle$ with period 6 to the antiphase $\langle 2 \rangle$ with period 4 in the previous result. In addition, the commensurate phases with periods $p = 9, 11, 17$ and 29 can be found in the set of modulated phases. Furthermore, we studied the variation of the wavevector with temperature in a modulated phase by using Lyapunov exponent associated with trajectory of the system. Finally, we found that stability of a limit cycle of period $p > 6$ can be found in a narrow interval in the modulated phase.

References

- [1] Wu F Y 1982 *Rev. Mod. Phys.* **54** 235
- [2] Akin H and Temir S 2011 *Cond. Matt. Phys.* **14** 23003
- [3] Akin H, Rozikov U A and Uguz S 2014 *Math. Phys. Anal. Geom.* **17** 103
- [4] Ganikhodjaev N, Akin H, Uguz S and Temir S 2011 *J. Stat. Mech. Theory Exp.* **2011** P03025
- [5] Ganikhodjaev N and Mohd Rodzhan M H 2015 *J. Kor. Phys. Soc.* **66** 1200-1206
- [6] Ganikhodjaev N and Mohd Rodzhan M H 2016 *Malaysian Journal of Mathematical Sciences* **10** 167-180
- [7] Ganikhodjaev N, Akin H and Temir S 2007 *Turk. J. Math.* **31** 229-238
- [8] Ganikhodjaev N, Mukhamedov F M and Pah C H 2008 *Appl. Phys. Letters.* **373** 33-38
- [9] Ganikhodjaev N, Nawi A M and Mohd Rodzhan M H 2012 *J. Kor. Phys. Soc.* **61** 998
- [10] Ganikhodjaev N, Temir S and Akin H 2009 *J. Stat. Phys.* **137** 701-715
- [11] Vannimenus J 1981 *Z. Phys. B.* **43** 141-148